FAULT CLASSIFICATION AND LOCATION IN MVDC SHIPBOARD POWER SYSTEMS USING EXTREME LEARNING MACHINE

Karthikeyan.M[a] , Rengaraj.R[b]

[a] Department of Electrical and Electronics Engineering, Velammal Engineering College, Chennai, India
[b] Department of and Electronics Engineering, SSN College of Engineering, Chennai, India
[a] Corresponding Author: M.Karthikeyan, E-Mail : eee.karthikeyan@velammal.edu.in, Tel: +919944100171

Abstract: *In this article, a new fault classification and location method for medium voltage direct current (MVDC) shipboard power systems is presented. Smooth and uninterrupted power supply in MVDC shipboard power systems requires an efficient fault classification and location method. A parametric technique called autoregressive (AR) signal modeling is used to extract features from the current signal for full cycle duration at the point of measurement. The AR coefficients of the modeled current signal are used as input for the fault classifier and fault locators. The proposed fault classifier and fault locators are designed using machine intelligent technique based on extreme learning machine (ELM). The proposed fault classifier and fault locator has been tested with 8640 and 6480 cases respectively with wide variation in system parameters. Test results indicate that the proposed method is simple, reliable, effective, and accurate than the existing method in fault classification and location for MVDC shipboard power systems.*

Keywords: *Autoregressive (AR) signal modeling; Fault detection, Fault classification, Fault location, Extreme learning machine (ELM)*

1. Introduction

Medium voltage direct current (MVDC) zonal distribution architecture is proposed as a new distribution system for the all-electric ships in which the presence of power converters is pervasive [1-2]. These power electronic devices can significantly simplify the system by providing more available space, possible cost reduction, higher efficiency, higher safety, and variable control to achieve self-healing and survivability [3]. However fault classification and location in MVDC shipboard power systems is a challenging task.

A traveling wave based fault locator is presented for accurate fault location on distributed overhead lines and underground cables [4]. Here, travelling time of the high-frequency voltage signal with a sampling rate of 200 MHz is used to determine the fault distance. However, the MVDC power system is of small scale, making it difficult to measure with enough accuracy the time difference of the traveling wave. Moreover in practical, real effect, such as cable terminations, junctions and terminal connections may impact the performance of the method. Artificial neural network (ANN)–based fault classification and location in MVDC shipboard power systems is presented in [5]. It is found to be efficient in detecting the type and location of direct current (DC) cable faults. However, it needs large training sets and the learning process is consuming time. A discrete wavelet transform based real-time detection of DC-link short-circuits faults have been employed in DC transit systems [6]. Here, fault detection is being carried out using a self-organizing neural network for which an extracted feature vector from current waveform is given as input.

Fault identification and classification of short medium voltage underground cables using ANN is presented in [7]. Here, voltage and current signals for a complete full cycle have been used to detect the fault. In [8], an application of wavelet transform to digital distance-protection of transmission lines is presented. The wavelet transform method uses a multi-resolution analysis of the line currents to calculate different wavelet coefficients that help in detecting the type of fault. An application of wavelet transform and ANN to MVDC shipboard power systems is presented in[9]. The network is trained and tested with only a few cases. The use of high-frequency components of the fault-generated transient signals was studied for fault protection [10] and this method enables accurate fault detection unaffected by power swings.

A fault location scheme using impedance-based and voltage matching method for unbalanced power distribution system in the presence of the distribution generation is presented in [11]. This scheme uses pre fault and during fault voltages and currents. The estimated error using this scheme lies between 0.001% and 0.1%. An active impedance estimation based fault location scheme is presented for a modern DC marine power distribution system [12]. Here, triangular current spikes are injected into the system once a short-circuit fault is detected. A fault location method for inter-line and grounded fault using one-terminal information based on distributed parameter model of double-circuit transmission line is presented in [13]. A traveling-wave-based method for wide-area fault location in multi terminal DC systems is presented in [14]. The first surge arrival time alone is needed for this method and it resulted with a maximum error of 0.176%. The location of DC line-faults in HVDC system is predicted based on traveling-wave natural frequency using half cycle current data from the single end [15]. This method has achieved an accuracy of less than 0.3% error under different fault conditions. An automated analysis approach using synchronized samples during transients from both the ends of the transmission line to locate transmission line faults is presented in [16]. This method can locate a fault with 3% accuracy. An analytical method based on only the voltage data of both ends of the faulted circuit is used for calculating the fault location for double-circuit transmission line [17]. The estimated error is less than 0.3% for different test cases using the voltage data. A fault location estimation algorithm based on analysis of measurements of voltage and current during discrete system states of single-phase and three-phase auto reclose scheme is presented in [18]. The fault location estimation error is less than 0.3% for this algorithm. A linear regression technique using the sample number at which wavelet coefficient details is greater than threshold is used for locating the transmission line faults [19]. The maximum estimation error associated with this linear regression technique is 0.75%.

The fault location estimation error lies between 0.001% and 3% for all the schemes discussed above. All these recent fault locators [11-19] motivate the researchers to design a fault locator with less % error. SVM based fault classifiers are used for fault detection and classification in electrical machines [20-21]. A number of practical applications of intelligent techniques using support vector machine for power system transient analysis have been reported [22–24]. Thus, it is necessary to develop a signal pattern analysis-intelligence technique based method for fault classification and fault location in MVDC shipboard power systems. The main objective of this work is to design a fault classifier with high classification accuracy and fault locator with less % error. In this paper, autoregressive-extreme learning machine (AR–ELM) is proposed and developed to classify and locate the fault in the MVDC shipboard power systems, thus supporting the decision on mitigating actions.

The rest of the article is organized as follows. Section 2 gives a brief description about the MVDC shipboard power system architecture. Section 3 introduces the proposed method. Section 4 presents auto regressive signal model. Section 5 presents brief review on extreme learning machine. Section 6 describes the fault classification and location in detail. Section 7 presents the results and discussion. Section 8 contains the conclusion of the paper.

2. MVDC Shipboard power system architecture

Fig. 1 shows the MVDC ship board architecture. A port distribution bus and star distribution bus are the two buses that run longitudinally along the ship. The network is distributed as five zones. There are two generators G_1, G_2 that are connected to Zone 1 and 2 through power electronic converters and circuit breakers. Zone 3 and 4 supplies vital and non vital loads respectively. Zone 5 consists of a radar load which is supplied from either of the MVDC buses through power electronic rectifier. The three types of DC fault that can occur in MVDC shipboard power system are (i) positive-rail-to-ground fault (PR–G), (ii) negative-rail-to-ground fault (NR–G) and (iii) rail-to-rail fault (R–R) [5].

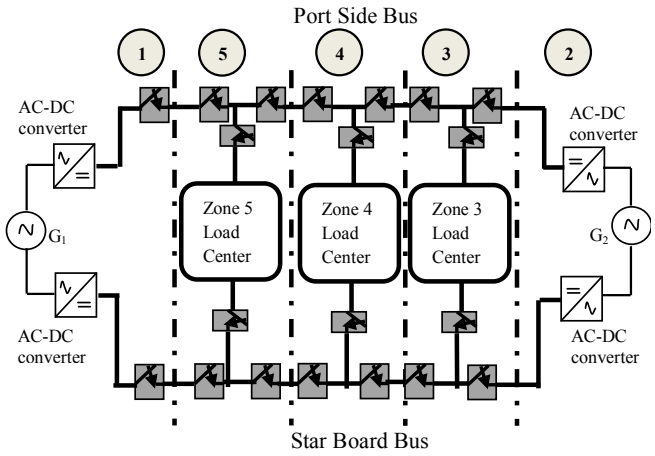

Fig.1. Architecture of MVDC shipboard power system.

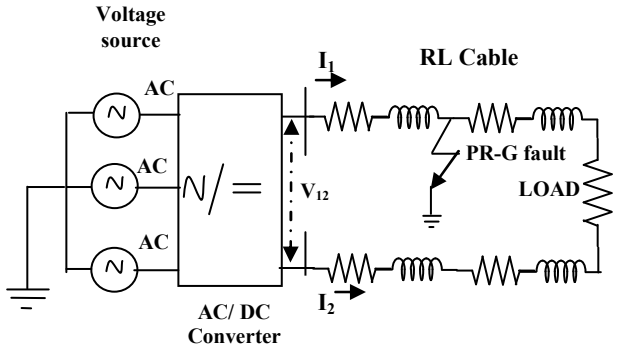

Fig. 2. Simulated equivalent MVDC shipboard power system.

An equivalent MVDC shipboard power system is shown in Fig.2. It is simulated using MATLAB to perform the proposed fault classification and location method. The developed MVDC power system is shown in Fig. 2. AC voltage source is converted into DC voltage (V_{12}) using an uncontrolled diode rectifier (AC/DC converter). It supplies the load through the RL cable whose length is 1 km. I_1 and I_2 represent the current on the DC lines. The parameters of the system are shown in Table I.

TABLE I
Parameters of simulated MVDC shipboard power system

AC voltage source	5.5 kV
Resistance of each cable	0.002 Ω
Inductance of each cable	40 µH
Load	5 Ω

The information obtained from the current waveforms (I_1, I_2) at the point of measurement is used to perform the fault classification and location task in the MVDC shipboard power system. Current waveform (I_1) at the point of measurement when a positive rail to ground (PR-G) fault occurs at 0.2 s with duration of the fault equal to five cycles is shown in Fig. 3. The current value rises quickly to a value greater than the value observed under the normal condition. The current signal for one cycle duration is modeled by the autoregressive signal modeling and the autoregressive coefficients are used to classify and locate the fault in MVDC shipboard power system.

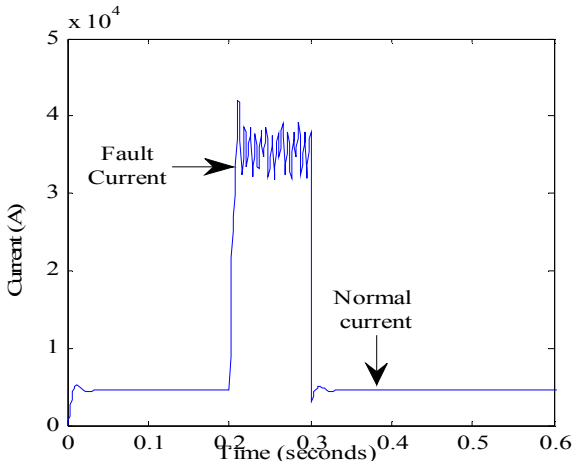

Fig. 3. Current waveform under normal and fault condition.

3. Proposed AR-ELM Method

The block diagram of the proposed method is shown in Fig. 4. A parametric method called the AR modeling is used to extract features from current signal of one cycle duration at the point of measurement. The AR coefficients of the fault current for one cycle duration are calculated after the occurrence of fault. These calculated AR coefficients are used as input for the fault classifier and fault locators. The fault classifier is designed to classify the four types of faults. They are AC fault (source fault) and the possible three DC faults (PR-G, NR-G, and R-R). When the output of the fault classifier is AC fault, then proper mitigating action should be taken on the source side. When the fault is classified as any one of the possible three DC faults (PR-G/NR-G/R-R), then the corresponding fault locator will be selected. The output of the fault locator is the fault distance from the point of measurement.

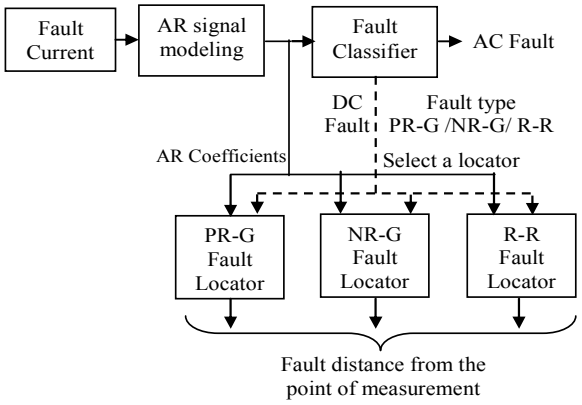

Fig. 4. Block diagram of the proposed AR-ELM method.

The prerequisite of the proposed AR-ELM method is that the fault should be detected. For detection of faults, a number of approaches have been proposed by different researchers [6-10]. Hence, a priori knowledge of accurate fault detection has been taken for granted.

4. Autoregressive signal modeling

The most commonly used methods for spectral analysis are nonparametric, such as fast Fourier transform (FFT) and discrete wavelet transform (DWT). FFT is characterized by poor spectral estimation. However, DWT has high frequency resolution but it cannot extract correct signal features during noisy conditions. DWT requires additional preprocessing to suppress noise. This section describes the basic theory for parametric modeling of signals using AR method. The AR signal modeling has found wide applications in the analysis of biomedical signals [25], fault detection and location in rotating machines due to bearing failure [26]. It is recently used as a powerful tool for power system disturbances analysis such as low frequency oscillations estimation [27] and islanding detection [28]. The AR modeling of the current signal $i(t)$ can be represented as the response of a linear time invariant system with white noise $e(t)$ as input, where the system is modeled by a finite number of poles. The AR(p) model of the current signal $i(t)$ at time t is defined as:

$$i(t) = -\sum_{j=1}^{p} a_j i(t-j) + e(t) \tag{1}$$

where a_j is the AR coefficients, $i(t-j)$ is the current signal $i(t)$ delayed by j samples and p is the number of pole. The AR coefficients are estimated using the traditional Yule-Walker method with the Levinson-Durbin recursion. Equation (1) can be expressed as a linear filter in the z-transform domain as:

$$I(z) = -I(z)\sum_{j=1}^{p} a_j z^{-j} + E(z) \tag{2}$$

Where $I(z)$ and $E(z)$ are the z-transforms of $i(t)$ and $e(t)$, respectively. The transfer function of all-pole system is:

$$H(z) = \frac{I(z)}{E(z)} = \frac{1}{1+\sum_{j=1}^{p} a_j z^{-j}} \tag{3}$$

The pole p_j can be calculated from the roots of the AR coefficient polynomial in the denominator of $H(z)$. Each pole p_j has a phase ϕ_j and a magnitude r_j, which is the distance of pole from the origin. The pole which moves closely to the origin is the critical pole [26]. The spectral power P_j of the pole p_j is calculated by multiplying real part of the residue term with the variance of the driving AR time series σ^2 and the scale factor n.

$$r_j = z^{-1}(z - p_j)H(z)\big|_{z=p_j} \tag{4}$$

$$P_j = \sigma^2 n Re(r_j)\big|_{z=p_j} \tag{5}$$

The AR model gives compressed data with smooth frequency spectrum without loss of essential features from the current signal. Fig. 5 shows the power spectrum density estimate (PSD) obtained using FFT and AR model of the current signal at the point of measurement for PR-G fault. Fig. 6 shows the AR coefficients of the current signal under normal and different fault conditions. The difference between coefficients for different types of fault and normal condition is apparent such that these coefficients can be given as input for fault classifier and fault locator to perform their task. This makes AR modeling as a proper feature extraction tool which leads to better classification and location accuracy.

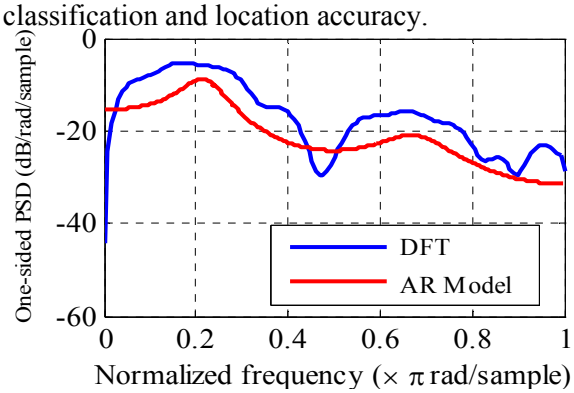

Fig. 5. Periodogram versus PSD estimation of the current signal for PR-G fault.

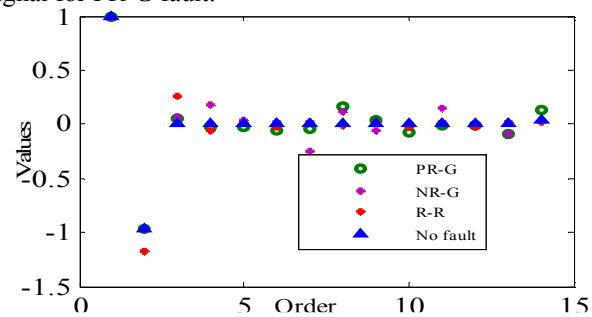

Fig. 6. AR coefficients of the current signal under normal and fault condition.

5. Extreme learning machine

Extreme learning machine (ELM) is a single hidden-layer feed forward neural network (SLFN) which provides efficient unified learning solutions for the applications of feature learning, clustering, regression and classification in engineering problems [29-31]. The learning speed of ELM is faster than the traditional feed-forward network learning algorithm like back propagation algorithm while obtaining better generalization performance. The architecture of ELM model is shown in Fig. 7. ELM randomly chooses and fixes the weights between input neurons and hidden neurons based on continuous probability density function, and then analytically determines the weights between hidden neurons and output neurons of the SLFN [32-34]. For N samples $\{(x_k, t_k)\}_{k=1}^{N}$, where input vector $x_k = [x_{k1}, x_{k2}, ..., x_{kn}]^T$ and target vector $t_k = [t_{k1}, t_{k2}, ..., t_{km}]^T$ a standard SLFN with $\tilde{N}$ hidden neurons and activation function $g(x)$ is mathematically modeled as:

$$\Sigma_{i=1}^{\tilde{N}} \beta_i g(w_i \cdot x_k + b_i) = O_k, k = 1,2,..., N \quad (6)$$

where $w_i = [w_{i1}, w_{i2}, ..., w_{in}]^T$ is the weight vector connecting the i^{th} hidden neuron and the input neurons, $\beta_i = [\beta_{i1}, \beta_{i2}, ..., \beta_{im}]^T$ is the weight vector connecting the i^{th} hidden neuron and the output neurons, $O_k = [O_{k1}, O_{k2}, ..., O_{kn}]^T$ is the output vector of the SLFN and b_i is the threshold of the i^{th} hidden neuron. $w_i \cdot x_k$ denotes the inner product of w_i and x_k. These N equations can be written compactly as:

$$H\beta = O \quad (7)$$

where

$$H = \begin{bmatrix} g(w_1 \cdot x_1 + b_1) & ... & g(w_{\tilde{N}} \cdot x_1 + b_{\tilde{N}}) \\ \vdots & ... & \vdots \\ g(w_1 \cdot x_N + b_1) & ... & g(w_{\tilde{N}} \cdot x_N + b_{\tilde{N}}) \end{bmatrix}_{N \times \tilde{N}} \quad (8)$$

$$\beta = \begin{bmatrix} \beta_1^T \\ \vdots \\ \beta_{\tilde{N}}^T \end{bmatrix}_{\tilde{N} \times m} \quad and \quad O = \begin{bmatrix} O_1^T \\ \vdots \\ O_N^T \end{bmatrix}_{N \times m} \quad (9)$$

Here, H is called the hidden layer output matrix.

The number of hidden neurons required to achieve a good generalization performance is much less. The resulting training error might not approach to zero but can be minimized by solving the following problem:

$$\min_{\beta} \left\| H(w_1, ..., w_{\tilde{N}}, b_1, ..., b_{\tilde{N}})\beta - T \right\|^2 \quad (10)$$

where target, $T = \begin{bmatrix} t_1^T \\ \vdots \\ t_N^T \end{bmatrix}_{N X m}$ (11)

ELM randomly assigns and fixes the input weights w_i and bias b_i based on some continuous probability distribution function in the case of learning a structured function, only leaving output weights β_i to be adjusted according to: $\min_{\beta} \|H\beta - T\|^2$.

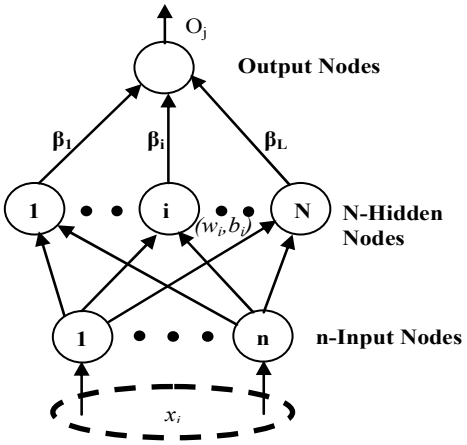

Fig. 7. Architecture of Extreme learning machine

The above problem is linear system optimization problem. Its unique least-squares solution with minimum norm is given by

$$\hat{\beta} = H^{\dagger}T, \quad (12)$$

where $H^{\dagger}$ is the Moore-Penrose generalized inverse of matrix H. The solution produced by ELM in (12) not only achieves the minimum square training error but also the best generalization performance on novel patterns. ELM can perform direct classification for multi-category problems in a fast and efficient manner.

6. Fault classification and location

A. Training and testing data set generation

To study the effectiveness of the proposed method under different conditions, different combinations of parameters have been considered. The training patterns are generated for three different types of fault (PR-G, NR-G, R-R) on the DC bus with ten locations, six fault resistances, two fault inception angles and two load resistances. Thus a total of 3 × 10 × 6 × 2 × 2 =720 cases have been generated for training. The training patterns are generated for 10 different types of AC fault for ABC phases (A-G, B-G, C-G, A-B, B-C, A-C, A-B-G, B-C-G, A-C-G and A-B-C) on the source side with two source impedances, two load resistances, three fault resistances, two load angles and one fault inception angle. Thus a total of 240 cases of AC side faults have been generated for training. The duration of the fault has been assumed to be five cycles. Therefore, the fault classifier is trained with 960 cases. They are 720 cases of DC fault and 240 cases of AC fault.

The testing patterns are generated for three different types of fault (PR-G, NR-G, R-R) on the DC bus with 90 locations, six fault resistances, two fault inception angles and two load resistances. Thus a total of 6480 cases for all the three DC faults have been generated for testing. The testing patterns are generated for 10 different types of AC fault on the source side with three source impedances, two load resistances, six fault resistances, three load angles and two fault inception angles. Thus a total of 2160 cases of AC faults on source side have been generated for testing. Therefore, the fault classifier is tested with 8640 cases. They are 6480 cases of DC fault and 2160 cases of AC fault.

Each of the three fault locators is trained with 240 cases and tested with 2160 cases of DC fault. Hence, a total of 6480 cases are tested using the three fault locators. The parameter values that have been chosen for training and testing are given in Table II & III.

TABLE II
Details of training and testing patterns for DC faults

Parameters	**Training**	**Testing**
Fault location (FL)	at distances of 10,20,…100% of DC bus length	at distances of 11,12,…100% of DC bus length
Fault resistance (R_f)	0.01, 0.2, 2, 5, 6, 10Ω	0.01,0.1,1,10,25, 50 Ω
Fault inception angle (FIA)	0º,90º	36º,72º
Load resistance (R_L)	1, 5Ω	1, 10 Ω

TABLE III
Details of training and testing patterns for AC faults

Parameters	**Training**	**Testing**
Source impedance (Z_S)	100%, 50%	75%, 100%, 125%
Load resistance (R_L)	1, 5Ω	1, 10 Ω
Fault resistance (R_f)	0.01, 1,10Ω	0.01,0.1,1,10,25, 50 Ω
Load angle (δ)	0º, 90º	0º, 60º, 90º
Fault inception angle (FIA)	0º	36º,72º

B. AR-ELM based fault classifier and fault locator

The current signals I_1, I_2 at the point of measurement sampled at a rate of 1 kHz for full cycle duration is modeled using AR signal modeling. The signal window of 20 ms and model order p = 13 are used for the AR coefficients calculation. The model order is selected using common rule that AR order should be around one third of the data window size [28]. The calculated thirteen AR coefficients are given as input to the ELM classifier which makes the number of input nodes equal to thirteen. AR-ELM fault classifier is a multiclass classifier that consists of four classes. Classes 1 to 3 correspond to DC faults (PR-G, NR-G, and R-R), and class 4 corresponds to AC fault. Therefore, number of output nodes is equal to four. The output of the fault classifier belongs to a particular class when the weight of that output node is greater than the other three nodes. The proposed fault classifier is able to discriminate source side AC fault from DC fault with the current at the point of measurement on the DC cable. The parameter to be selected for the AR-ELM fault classifier is the number of hidden nodes. The number of hidden nodes is increased from one by a step of one during training until the optimal number of nodes is selected based on cross-validation with a training accuracy equal to one. The number of hidden nodes obtained when AR-ELM classifier is trained with 960 cases is 72 for sigmoid activation function. Fig. 8 shows the selection of number of hidden nodes for AR-ELM classifier. The performance evaluation criterion for fault classifier is the classification accuracy and it is given by:

$$\%\,classification\ accuracy = \frac{True\ \ fault\ \ classification}{Number\ of\ \ test\ \ cases} \times 100 \qquad (13)$$

Based on the output of the fault classifier, any one of the fault locator will be selected. The thirteen AR coefficients of the fault current signal are given as input to the fault locator modules. AR-ELM fault locator considers the fault location task as a

regression case. Therefore, the number of output node is equal to one. The weight of the output node gives the distance of the fault from the point of measurement.

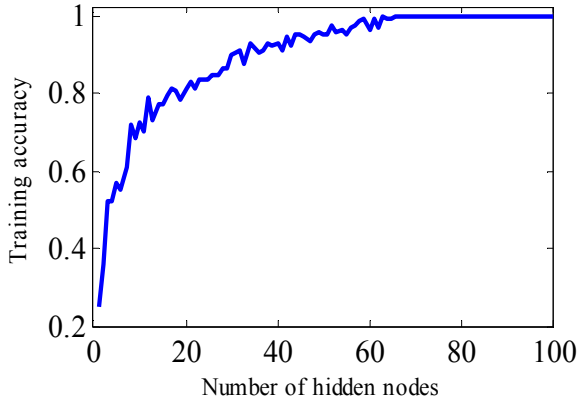

Fig. 8. Training accuracy vs. number of hidden nodes.

The parameter to be selected for the AR-ELM fault locator is the number of hidden nodes. The number of hidden nodes is increased from one by a step of one during training until the optimal number of hidden nodes is selected based on cross-validation with the root mean square error (RMSE) equal to 0.0005. The number of hidden nodes obtained when AR-ELM fault locator is trained with 240 cases is 88, 96, and 116 for sigmoid activation function. Fig. 9 shows the selection of number of hidden nodes for AR-ELM fault locators.

The criterion for evaluating the performance of the fault locator is defined as

$$\%error = \frac{\left| Fault\ locator\ output - Actual\ fault\ location \right|}{Total\ length\ of\ the\ DC\ cable} \times 100 \quad (14)$$

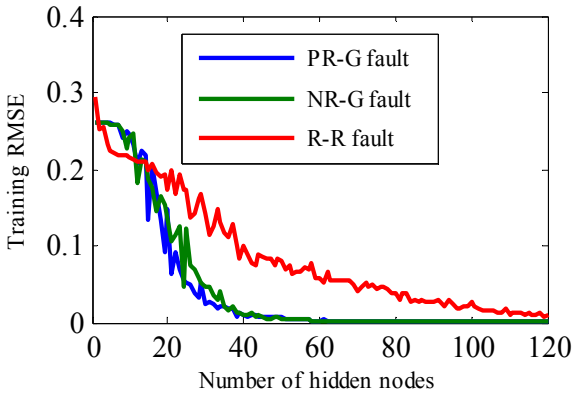

Fig. 9. RMSE vs number of hidden nodes

7. Results and Discussions

The AR-ELM fault classifier is tested with 8640 test cases. An overall classification accuracy of 99.7% has been obtained by the proposed method. Table IV depicts the performance of the proposed fault classification method for different types of faults. It is inferred from Table IV that the proposed method gives highly accurate results for all the types of faults.

TABLE IV
Fault classification accuracy for different fault types

Fault Type	No. of test cases	No. of misclassification	No. of true classification	Accuracy (%)
PR-G	2160	-	2160	100
NR-G	2160	-	2160	100
R-R	2160	26	2134	98.8
AC	2160	-	2160	100
Total	8640	26	8614	99.7

The breakup of the classification results obtained during testing is given in Table V. The diagonal elements represent the correctly classified faults and the off-diagonal elements represent the misclassification. The total true fault classification is 8614 test cases. The overall classification accuracy of the AR-ELM fault classifier is 99.7%.

TABLE V
Classification results of AR-ELM fault classifier

Fault Type	PR-G	NR-G	RR-G	AC
PR-G	**2160**	-	-	-
NR-G	-	**2160**	-	-
R-R	16	-	**2134**	10
AC	-	-	-	**2160**

From Tables IV & V it is observed that even with a small training data (which is roughly 11% of the test data), the classification accuracy of the proposed method is high. Of the total 2160 R-R fault test cases, 16 are misclassified as PR-G fault and 10 are misclassified as AC fault. The details of the 26 misclassified test cases are given in Table VI. The 26 misclassified test cases have R_f =0.01Ω. But, all the test cases of PR-G, NR-G, and AC faults with fault resistance R_f =0.01Ω have been classified correctly.

For the test cases 1-10 given in Table VI, the output of node 4 is greater than other three nodes. Hence, the output of fault classifier is AC fault.

TABLE VI
Details of the misclassified test cases of the AR-ELM fault classifier

S.No	Fault location (p.u)	Fault resistance (Ω)	Load resistance (Ω)	Fault Inception angle	Output of node 1	Output of node 2	Output of node 3	Output of node 4	Predicted fault type
1	0.12	0.01	1	36º	-4.3922	-4.2463	2.8212	3.8178	AC
2	0.12	0.01	1	72º	-4.3921	-4.2462	2.8215	3.8172	AC
3	0.13	0.01	1	36º	-4.8024	-4.5998	3.1201	4.2826	AC
4	0.13	0.01	1	72º	-4.8023	-4.5997	3.1205	4.2819	AC
5	0.14	0.01	1	36º	-5.018	-4.6891	3.3369	4.3706	AC
6	0.14	0.01	1	72º	-5.0179	-4.689	3.3374	4.3699	AC
7	0.15	0.01	10	36º	-4.9976	-4.5408	3.4149	4.1239	AC
8	0.15	0.01	10	72º	-4.9975	-4.5406	3.4154	4.1231	AC
9	0.16	0.01	1	36º	-4.7266	-4.193	3.3227	3.5973	AC
10	0.16	0.01	1	72º	-4.7265	-4.1928	3.3232	3.5965	AC
11	0.21	0.01	10	36º	0.2625	-0.4818	-0.1606	-1.6201	PR-G
12	0.21	0.01	10	72º	0.2626	-0.4805	-0.1626	-1.6195	PR-G
13	0.22	0.01	1	36º	1.049	0.0932	-0.0726	-3.0698	PR-G
14	0.22	0.01	1	72º	1.049	0.0934	-0.0718	-3.0708	PR-G
15	0.22	0.01	10	36º	1.44	-0.0565	-1.2965	-2.0871	PR-G
16	0.22	0.01	10	72º	1.4401	-0.0547	-1.2988	-2.0867	PR-G
17	0.23	0.01	1	36º	1.6171	0.5015	0.0234	-4.1423	PR-G
18	0.23	0.01	1	72º	1.6177	0.5019	0.0233	-4.1432	PR-G
19	0.23	0.01	10	36º	2.5866	0.414	-2.4408	-2.5599	PR-G
20	0.23	0.01	10	72º	2.587	0.4159	-2.4448	-2.5583	PR-G
21	0.24	0.01	10	36º	2.313	0.2237	-1.8436	-2.6932	PR-G
22	0.24	0.01	10	72º	2.32	0.2289	-1.8561	-2.693	PR-G
23	0.25	0.01	10	36º	1.2763	-0.326	-0.5326	-2.4179	PR-G
24	0.25	0.01	10	72º	1.2827	-0.3209	-0.5433	-2.4186	PR-G
25	0.26	0.01	10	36º	0.4483	-0.7244	0.3016	-2.0257	PR-G
26	0.26	0.01	10	72º	0.454	-0.7197	0.2927	-2.0272	PR-G

For test cases 11-26, the output of node 1 is greater than the other three nodes. Hence, the output of the fault classifier is PR-G fault. In all the 26 test cases, the output of node 3 should have been greater than the other three nodes to classify these test cases as R-R fault. The misclassified test cases belong to the fault location that lies between 12 to 16% and 21 to 26% of the cable length. This indicates the severity of the short kilometric fault affecting the accuracy of the AR-ELM fault classifier from achieving 100%.

Each of the three fault locators is tested with 2160 test cases. The output of the fault locator is the distance of the fault from the point of measurement in per unit. The performance of the fault locators are evaluated using equation (14). Table VII gives the test results of the AR-ELM fault locators for different fault cases of the system. These ten cases correspond to descending order of % error of the fault locators in the total 6480 test cases. The minimum, maximum, mean error and standard deviation for the three fault locators are given in Table VIII. The maximum error of the PR-G and R-R fault locator corresponds to the first two test cases of Table VII. The maximum error of the PR-G fault locator is 0.04219% which is less than maximum error of 4.86% of the artificial neural network based fault locator reported in [5].

TABLE VII
Test results of the AR-ELM fault locators

Fault Type	Fault Location (p.u.)	Fault Resistance (Ω)	Load Resistance (Ω)	Output of fault locator (p.u)	% error of fault locator
PR-G	0.1	0.1	10	0.10042	0.04219
R-R	0.68	0.01	10	0.68033	0.03345
PR-G	0.52	0.01	1	0.52027	0.02759
R-R	0.54	0.01	1	0.53973	0.02677
PR-G	0.52	0.01	1	0.52026	0.02618
PR-G	0.5	0.01	1	0.49974	0.02610
PR-G	0.1	1	1	0.10025	0.02544
PR-G	0.5	0.01	1	0.49975	0.02520
R-R	0.88	0.01	10	0.88025	0.02512
R-R	0.53	0.01	1	0.52977	0.02262

TABLE VIII
Performance of the AR-ELM fault locators

Type of locator	Minimum error (%)	Maximum error (%)	Mean error (%)	Standard deviation
PR-G	9.6555e-007	0.0422	0.0034	0.0035
NR-G	1.8161e-007	0.0210	0.0027	0.0026
R-R	5.6117e-006	0.0334	0.0036	0.0033

The probability density curve of % error of the three fault locators are shown in Fig.10 and its distribution is given in Table IX. As observed from Table IX, the three fault locators predicted the fault location with less than 0.01% error for 6238 (96.27% of test data). It is observed that even with a small training data (which is roughly 11% of the test data), the fault locator accuracy of the proposed method is high.

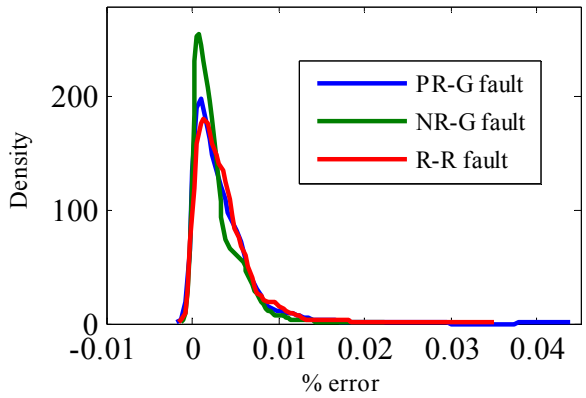

Fig.10. Percentage error density curve of fault locators

TABLE IX
% error distribution for AR-ELM fault locators

% error Range	Type of fault locator: PR-G fault locator	NR-G fault locator	R-R fault locator	Total test samples
0.0-0.005	1652	1794	1639	5085
0.005-0.01	406	327	420	1153
0.01-0.015	70	33	71	174
0.015-0.02	23	5	21	49
>0.02	9	1	9	19
Total	2160	2160	2160	6480

The effect of the fault distance on the performance of the fault locators is analyzed by calculating % mean error on each fault location. The total 6480 test cases consist of 90 locations with 72 test cases in each location. The mean error of these 72 test cases are calculated for each fault location and plotted against the fault distance as shown in Fig.11. The distribution of this mean error is uniform throughout the entire length of the cable considered.

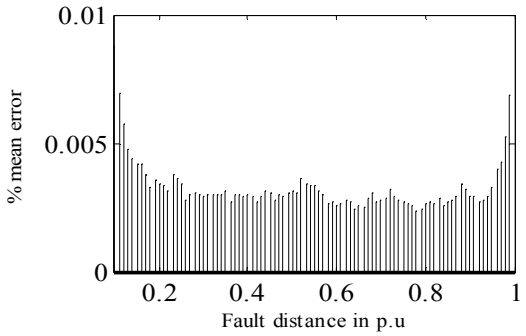

Fig.11. Effect of fault distance on the performance of fault locator

The effect of the fault resistance on the performance of the fault locators is analyzed by calculating % mean error for three fault resistances on each fault location. The total 6480 test cases consist of 90 locations with six fault resistances. So, for each fault resistance, the fault locators are tested with 12 test cases in each location. The mean error of these 12 test cases are calculated for each fault location and plotted against the fault distance as shown in Fig.12. The three fault resistances considered are $R_f = 0.01, 1, 10\,\Omega$. The performance of the fault locator is unaffected by the fault resistance as the % mean error is less in all the three cases considered.

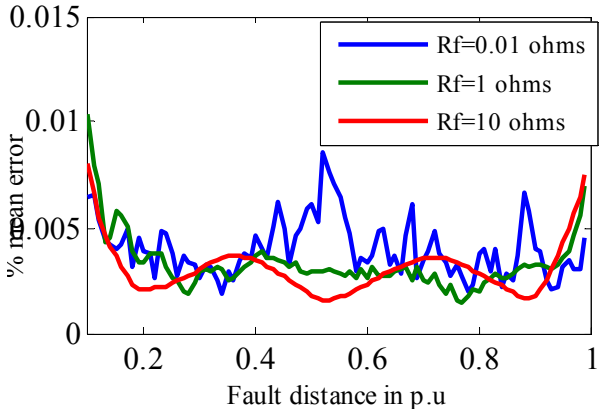

Fig.11. Effect of fault resistances on the performance of fault locator

The proposed AR-ELM fault classifier performed efficiently in classifying the fault with negligible error when tested with 8640 test cases. The proposed AR-ELM fault locators predicted the fault distance from the point of measurement with less % error when tested with 6480 test cases.

A. *Further studies*

The performance of the proposed AR-ELM fault classifier is analyzed by changing the data window size. The current signals I_1, I_2 at the point of measurement sampled at a rate of 1 kHz for half cycle duration is modeled using AR signal modeling. The signal window of 10 ms and model order $p = 6$ are used for the AR coefficients calculation. The calculated six AR coefficients are given as input to the fault classifier. Table X depicts the performance of the fault classifier for half cycle duration of current signal. The classification accuracy obtained is 98.96% which is little lower than the accuracy obtained by using full cycle duration current samples. But, the accuracy obtained by using the half cycle duration current samples can also be considered as a satisfactory one.

TABLE X
Fault classification accuracy for different fault types for half cycle duration

Fault Type	No. of test cases	No. of misclassification	No. of true classification	Accuracy (%)
PR-G	2160	-	2160	100
NR-G	2160	-	2160	100
R-R	2160	90	2070	95.83
AC	2160	-	2160	100
Total	8640	90	8550	98.96

B. *Comparison with other scheme*

Recently, a method that integrates wavelet transforms (WT)-based multi resolution analysis technique with artificial neural network (ANN) for fault detection and fault classification in MVDC shipboard power systems has been proposed in [9]. A classification accuracy of 99.58% had been reported with 160 training cases and 240 test cases [9]. For comparing the performance of the proposed AR-ELM fault classifier and locator with that proposed method in [9], fault classification and fault location task has also been carried out for all the test cases. MATLAB-Neural network toolbox is used for the ANN implementation. The db10 wavelet and scale 9 are chosen as the mother wavelet. The DWT of the current signals of one cycle duration are found out. The wavelet coefficients are given as input for the fault classifier and locator designed using ANN. WT-ANN fault classifier is tested with 8640 test cases. The overall classification accuracy of the fault classification method of [9] is 99.56% which is almost the same obtained by the proposed AR-ELM fault classifier. Table XI depicts the performance of the scheme of [9].

TABLE XI
Performance of the scheme of Ref. [9] for different fault types

Fault Type	No. of test cases	No. of misclassification	No. of true classification	Accuracy (%)
PR-G	2160	-	2160	100
NR-G	2160	-	2160	100
R-R	2160	28	2132	98.7
AC	2160	30	2130	98.6
Total	8640	58	8602	99.56

WT-ANN fault locators are test with 6480 test cases. The minimum, maximum, mean error and standard deviation for the three WT-ANN fault locators are given in Table XII. The maximum error of the WT-ANN fault locators is higher than maximum error of proposed AR-ELM fault locators.

TABLE XII
Performance of the WT-ANN fault locators of Ref. [9]

Type of locator	Minimum error (%)	Maximum error (%)	Mean error (%)	Standard deviation
PR-G	7.0541e-004	1.7554	0.2953	0.2019
NR-G	0.0014	1.2560	0.2609	0.1333
R-R	0.0026	1.3654	0.2708	0.1968

The performance of the WT-ANN classifier and AR-ELM classifier are almost the same. But the performance of the WT-ANN fault locators are poor than the AR-ELM fault locators. Since the maximum error for the WT-ANN fault locators are 1.7554%, 1.256%, and 1.3654% for PR-G, NR-G, R-R fault locators respectively, whereas the maximum error for the AR-ELM fault locators are 0.0422, 0.0210, and 0.0334%. The training and testing time required for the AR-ELM fault classifier and fault locators are very few minutes. But, WT-ANN fault classifier and fault locators needs several minutes. Hence, the proposed AR-ELM fault locators can be considered superior to the WT-ANN fault locators.

Also, ELM has better scalability and much better generalization performance at a faster learning speed (up to thousands of times) than traditional support vector machine (SVM) and least square support vector machine for the standard data sets as reported in [34]. So, SVM based fault classifier and locators are not taken into account for comparison of the performance of the proposed method. The performance of the AR-ELM fault classifier and fault locators are unaffected by parameter variations.

Hence, AR-ELM fault classifier and fault locators can be considered quite suitable for digital protection of the MVDC shipboard power systems.

8. CONCLUSION

AR-ELM based fault classification and location method for MVDC shipboard power systems is presented in this paper. Current signal for full cycle duration is modeled using AR signal modeling. The calculated AR coefficients of the fault current signal at the point of measurement are used as input to the fault classifier and fault locators. AR-ELM fault classifier is trained with 960 cases and tested with 8640 cases. Each of the three AR-ELM fault locators is trained with 240 cases and tested with 2160 test cases. The overall classification accuracy of AR-ELM fault classifier is 99.7%. AR-ELM fault locators performed accurately in locating the fault with less than 0.05% error. The maximum error obtained is 0.0422% by the PR-G fault locator. The three fault locators predicted the fault location with less than 0.01% error for 96.27% of test data. Hence, it is observed that the proposed fault classification and location method using AR-ELM is accurate and robust to parameter variation. The proposed method can be considered quite suitable scheme for the complete digital protection of MVDC shipboard power systems.

REFERENCES

1. M. E. Baran and N. Maharajan.: *System reconfiguration on shipboard DC zonal electrical system*. In: Proceedings of the IEEE Electric Ship Technologies Symposium, p. 86-92, July 25-27,2005, Philadelphia,USA.
2. M.Razvan, A.Mihaela.: *Advanced electric ship propulsion.* In: Journal of Electrical Engineering, Vol.9(2009), No.1, 2009, p.133-138
3. T. Ericsen, N. Hingorani, and Y. Khersonsky : *Power electronics and future marine electrical systems.* In: IEEE Transactions on Industrial Applications, Vol. 4(2006), No.1, Jan. 2006, p. 155-163,
4. Z. Q. Bo, G. Weller and M. A. Redfern: *Accurate fault location technique for distribution system using fault-generated high-frequency transient voltage signals.* In:IEE Generation Transmission Distribution, Vol.146(1999), No.1, Jan. 1999, p.73-79.
5. N. K. Chanda and Y. Fu.: *ANN-based fault classification and location in MVDC shipboard power systems.* In: Proceeding of the North American Power Symposium, p.1-7, Aug. 2011, Boston,USA.
6. C. S. Chang, S. Kumar, B. Liu, and A. Khambadkone: *Real-time detection using wavelet transform and neural network of short-circuit faults within a train in DC transit systems.* In: IEE Electric Power Applications, Vol.148(2001) , No. 3, May 2001, p. 251-256.
7. Marouf Pirouti, Amin A.Fatih, Ibrahim B.Sadik : *Fault identification and classification for short medium voltage underground cable based on artificial neural networks.* In: Journal of Electrical Engineering, Vol.59(2008), No.5,2008, p. 272-276.
8. Osman A.H. and Malik O.P.: *Transmission line protection based on wavelet transform.* In: IEEE Transactions on Power Delivery, Vol.19(2004), No.2, Apr. 2004, p.515-523.
9. Weilin Li, Antonello Monti, Ferdinanda Ponci: *Fault detection and classification in medium voltage DC shipboard power systems with wavelets and artificial neural networks*. In: IEEE Transactions on Instrumentation and Measurement, Vol.63(2014), No.11, oct. 2014, p. 2651-2665.
10. N.Zhang and M.Kezunovic: *Transmission line boundary protection using wavelet transform and neural network.* In: IEEE Transactions on Power Delivery, Vol.22(2007), No. 2, Apr. 2007, p. 859-869.
11. S.F.Alwash,V.K.Ramachandramurthy,N.Mithulananthan.: *Fault location scheme for power distribution system with distributed generation.* : In: IEEE Transactions Power Delivery, Vol.30(2015), No.3, June 2015, p. 1187-1195.
12. Ke.Jia, Tianshu Bi, Bohan Liu, Edward Christopher, David W.P.Thomas, Mark Sumner.: *Marine power distribution system fault location using a portable injection unit.* In: IEEE Transactions on Power Delivery, Vol.30(2015), No.2, April 2015, p. 818-826.
13. Jing Ma, Yuxin Shi, Wei Ma, Zengping Wang.: *Location method for inter-line and grounded fault using one-terminal information based on distributed parameter*.In: IEEE Transactions on Power Delivery, Vol.30(2015), No.3, Jul 2015, p. 1307-1316.
14. Sadegh Azizi, Majid Sanaye-Pasand, Moein Abedeni, Abbas Hasani.: *A traveling-wave –based method for wide-area fault location in multi terminal DC systems*. In: IEEE Transactions on Power Delivery, Vol.29(2014), No.6, Dec 2014, p. 2552-2560.
15. Zheng-You He, Kai Liao, Xiao-Peng Li, Sheng Lin, Jian-Wei Yang, Rui-Kun Mai.: *Natural frequency-based fault location in HVDC lines.* In: IEEE Transactions on Power Delivery, Vol.29(2014), No.2, April 2014, p. 851-859.
16. Papiya Dutta, Ahad Esmaeilian, Mladen Kezunovic.: *Transmission-line fault analysis using synchronized sampling.* In: IEEE Transactions on Power Delivery, Vol.29(2014), No.2, April 2014, p. 851-859.
17. Behnam Mahamedi, Jian Guo Zhu.: *Unsynchronized fault location based on the nagative-sequence voltage magnitude for double-circuit transmission lines.* In: IEEE Transactions on Power Delivery, Vol.29(2014), No.4, August 2014, p. 1901-1908.
18. Liang Ji, Campbell Booth, Adam Dysko, Fumio Kawano, Phil Beaumont.: *Improved fault location through analysis of system parameters during autoreclose operations on transmission lines.* In: IEEE Transactions on Power Delivery, Vol.29(2014), No.6, December 2014, p. 2430-2438.
19. G.Preethi, N.M.Rabindra.: *An approach for location of transmission line faults by wavelet analysis.* In: Journal of Electrical Engineering, Vol.13(2013). No.1, 2013, p.64-71.
20. U.J.Anjali, G.M.Dhole, S.R.Paraskar, B.Mirza Ansar.: *Signal processing based svm classifier for mixed fault detection in induction motor*. In: Journal of Electrical Engineering, Vol.13(2013). No.2, 2013, p.102-108.
21. A. Y. Hatata, A. El-Saeed, M. S. kandil.: *Power transformer condition monitoring and fault diagnosis*

using support vector machine. In: Journal of Electrical Engineering, Vol.15(2015), No.1, 2015, p.214-221.

22. Thukaram.D, Khincha .H.P and Vijaynarasimha H.P.: *Artifical neural network and support vector machine for locating faults in radial distribution systems.* In: IEEE Transactions on Power Delivery, Vol.20(2005), No.2, Apr. 2005, p.710-721.
23. Salat.R and Osowski.S.: *Accurate fault location in the power transmission line using support vector machine approach*. In: IEEE Transacations on Power Systems, Vol.19(2004) , No.2, Apr. 2004, p. 976-986.
24. Moulin L.S, Da Silva A.P.A, El-Sharkawi M.A and Marks R.J.II, *Neural networks and support vector machines applied to power systems transient stability analysis*, In: International Journal of Engineering Intelligent Systems, Vol.9(2011), No.4, oct.2011, p. 205-211.
25. M.Kiymikb, M.Akinc, and A.Alkanb.: *AR spectral analysis of EEG signals by using maximum likelihood estimation*. In: Computers in Biology and Medicine,Vol. 31(2001), No. 6, 2001, p. 441-450.
26. Suguna Thanagasundram, Sarah Spurgeon, Fernando Soares Schlindwein.: *A Fault detection tool using analysis from an autoregressive model pole trajectory*. In: Journal of Sound and Vibration Vol.317(2008), No.3, Nov. 2008, p. 975-993.
27. R.W.Wires, J.W.Pierre and D.J.Trudnowski. : *Use of ARMA block processing for estimating stationary low-frequency electromechanical modes of power systems*. In: IEEE Transactions on Power System, Vol.18(2003), No. 1, Feb. 2003, p.167-173.
28. Biljana Matic-Cuka, Mladen Kezunovic.: *Islanding detection for inverter-based distributed generation using support vector machine method*. In: IEEE Transactions on Smart Grid, Vol.5(2014), No. 6, Nov.2014, p.2676-2686.
29. Rahul.Dubey,S.R.Samataray, B.K.Panigrahi.: *An extreme learning machine based fast and accurate adaptive distance relaying scheme.* In: International Journal of Electrical Power and Energy Systems, Vol.73(2015), Dec. 2015, p.1002-1014.
30. Rahul.Dubey,S.R.Samataray, B.K.Panigrahi, Vijendran G.Venkoparao.: *Extreme learning machine based adaptive distance relaying scheme for static synchronous series compensator based transmission lines*.In: International Journal of Electric Power Components and Systems, Vol. 44(2016), No.2, 2016, p.219-232.
31. Y.Chen, E.Yao, and A.Basu.: *A 128 channel Extreme learning machine based neural decoder for brain machine interfaces.*In: IEEE Transactions on Biomedical Circuits and Systems, Vol.10(2016), No.3, June 2016, p.679-692.
32. Guang-Bin Huang, Qin-Yu Zhu and Chee-Kheong Siew.: *Extreme learning Machine: Theory and applications*. In: Neurocomputing, Vol.70(2006), 2006, p.489-501.
33. Guang-Bin Huang, Qin-Yu Zhu and Chee-Kheong Siew.: *Universal approximation using incremental constructive feedforward networks with random hidden nodes.*In: IEEE Transactions on Neural Networks, Vol.17(2006), No.4, 2006, p.879-892,.
34. Guang-Bin Huang, H.Zhou, X.Ding and R.Zhang.: *Extreme learning machine for regression and multiclass Classification*.In: IEEE Transactions on Systems Man , and Cybernetics – PartB: Cybernetics, Vol. 42(2012), No.2, 2012, p.513-529.